High-magnetic-field study of the phase transitions of $R_{1-x}Ca_xMnO_3$ (R=Pr, Nd)

M. Tokunaga* and N. Miura
Institute for Solid State Physics, University of Tokyo, Roppongi, Minato-ku, Tokyo 106, Japan

Y. Tomioka
Joint Research Center for Atom Technology (JRCAT), Tsukuba 305, Japan

Y. Tokura
Joint Research Center for Atom Technology (JRCAT), Tsukuba 305, Japan
and Department of Applied Physics, University of Tokyo, Tokyo 113, Japan
(Received 10 February 1997; revised manuscript received 8 September 1997)

We have investigated the magnetic-field-induced phase transitions of $R_{1-x}Ca_xMnO_3$ (R=Pr and Nd, x=0.50, 0.45 and 0.50, 0.45, 0.40) by measurements of magnetization, magnetoresistance, and magnetostriction utilizing a nondestructive long-pulse magnet (generating up to 40 T). We observed processes where magnetic fields destroy the real-space ordering of the charge carriers and cause insulator-to-metal phase transitions over the whole temperature region below about 250 K. We found that the destruction of the charge ordering is accompanied with a structural phase transition as well as with the magnetic phase transition and the colossal magnetoresistance effect. The different profiles of the temperature vs transition field curve depending on the carrier concentration x may be ascribed to the difference in the entropy between the commensurate and the discommensurate charge-ordered state. It turned out that the stability of the charge-ordered state is strongly correlated with the colinear antiferromagnetic ordering of the localized Mn moments. [S0163-1829(98)01509-4]

I. INTRODUCTION

Recently, perovskite-type manganites, $R_{1-x}A_xMnO_3$ (R and A are trivalent rare-earth ions and divalent alkaline-earth ions, respectively), have attracted considerable attention due to the colossal magnetoresistance (CMR) effect.[1–6] The mother material $RMnO_3$ is a kind of Mott insulators, and the Mn^{3+} ions have an electron configuration $t_{2g}^3e_g^1(S=2)$. Substitution of R^{3+} with A^{2+} produces holes in the e_g orbital and causes an insulator-metal transition, e.g., in the $La_{1-x}Sr_xMnO_3$ with an increase of x above 0.17.[4,7] The metallic $La_{1-x}Sr_xMnO_3$ ($0.17 \leqslant x \leqslant 0.60$) is a ferromagnet due to the double exchange (DE) interaction and exhibits the CMR effect only around the Curie temperature. This CMR effect has been explained in terms of the strong on-site (Hund's-rule) coupling between localized spins $S=\frac{3}{2}$ in the t_{2g} orbital and itinerant carriers in the e_g orbital. In some of the $R_{1-x}A_xMnO_3$ system with the ionic radii for the R and A sites being relatively small, however, the hole-doping does not produce the ferromagnetic metallic state.[8] As an earlier diffraction study[9] has revealed, a 1/1 ordering of Mn^{3+}/Mn^{4+} (charge ordering) appears in $La_{1-x}Ca_xMnO_3$ ($x \sim 0.5$). In $Pr_{1-x}Ca_xMnO_3$ in which the average ionic radius of the (R,A) cations is smaller, a similar charge-ordered (CO) state is realized in much broader regions. Jirák *et al.*[10] performed powder-neutron-diffraction measurements for the CO systems $Pr_{1-x}Ca_xMnO_3$. They found that a structural phase transition similar to that of $x=0.5$ takes place for $0.3 \leqslant x \leqslant 0.75$ at the charge-ordering transition temperature (T_{CO}). For $x=0.5$, the superstructure that doubles the orthorhombic unit cell in the [010] direction has been observed for the diffraction pattern at liquid He temperature.[10] Even for $x=0.3$, a similar superstructure has been observed below T_{CO} in the recent neutron-diffraction study.[8] This superstructure originates from the concomitant ordering of the e_g orbitals, which favors the charge exchange (CE)-type antiferromagnetic (AFM) spin ordering.[9]

Application of magnetic fields causes the destruction of the charge ordering. Tomioka *et al.* have reported the magnetoresistance measurements in $Pr_{1-x}Ca_xMnO_3$ ($0.30 \leqslant x \leqslant 0.50$) in magnetic fields up to 12 T.[11] The entire CO phase boundaries were determined for $x=0.35$ and 0.40 in the magnetic field (H) vs temperature (T) plane. A remarkable feature of these phase diagrams is that at low temperatures the transition field decreases with decreasing temperature. As a result, reentrance to the charge-disordered state or metallic state takes place by lowering temperature. These reentrant transitions have not been observed for other CO manganites $Nd_{1-x}Sr_xMnO_3$ (Ref. 12) or $Pr_{1-x}Sr_xMnO_3$ (Ref. 13) with $x=0.50$.

In the present work, we have studied the magnetic-field-induced phase transitions of the CO manganites in pulsed magnetic fields up to 40 T. Measurements of magnetization (M), magnetoresistance (MR), and magnetostriction have been carried out over a wide temperature range for $Pr_{1-x}Ca_xMnO_3$ and $Nd_{1-x}Ca_xMnO_3$. On the basis of these results, we could determine a full set of the CO phase diagrams and discuss the x-dependent behavior of the CO phase diagrams and the mechanism of the phase transition.

II. EXPERIMENT

$R_{1-x}Ca_xMnO_3$ (R=Pr and Nd) crystals were synthesized by the floating zone method, as detailed in Ref. 11. A part of

the rod was crushed and characterized by x-ray powder diffraction. The lattice parameters were estimated by the Rietveld refinement, which indicated that the Ca content in the obtained crystal systematically changes[14,15] according to the prescribed ratio. The inductively-coupled plasma mass spectrometry was also carried out to check the cation ratio R/Mn of the crystal. The result revealed that the ratio was almost in accord with the prescribed one within an accuracy of 2%. To check the possible oxygen deficiency for the highly doped crystals, the average Mn valence was checked by the redox titration technique.[16] It was estimated to be $+3.51$ for both $Pr_{1-x}Ca_xMnO_3$ ($x=0.50$) and $Nd_{1-x}Ca_xMnO_3$ ($x=0.50$).

By using a nondestructive long-pulse magnet[17] energized by a 200 kJ capacitor bank, we produced pulsed magnetic fields up to 40 T with a duration time of 11 ms. For magnetization (M) measurements, we used the induction method by employing a couple of coaxial pickup coils.[18] The inner coil had a diameter of 4.2 mm and 480 turns, while the outer coil had a diameter of 6.0 mm and its number of turns was adjusted to cancel the voltage induced in the inner coil by the magnetic fields. The voltage induced in the pickup coils was integrated numerically to obtain M. Transport measurements were carried out by the standard four-probe method with a dc current parallel to H (longitudinal magnetoresistance). The MS along the direction of H was measured by the capacitance method.[19] An optically flat Al-sputtered glass plate with a diameter of 7 mm was used for an electrode. The change of the sample length was measured by the change of a capacitance in the gap between the glass plate electrode and one side face of the sample where the electrode was attached. The gap was about 90 μm, and the capacitance was measured by a capacitance bridge with a frequency of 200 kHz. Those measurements were carried out in the temperature range from 1.4 K to room temperature.

III. RESULTS

A typical magnetization curve of a $Pr_{1-x}Ca_xMnO_3$ ($x=0.50$) crystal is shown in Fig. 1 as a function of H. At 1.4 K, charge-carriers take the CO state, and localized spins also order antiferromagnetically in zero magnetic field. With application of H, the M increases moderately up to about $1.3\mu_B$, and then jumps at 25 T, reaching a higher value ($\sim 3.7\mu_B$/Mn site) at 30 T. In the down-sweep process, the M stays at the high value for a field down to 20 T. The existence of the hysteresis is characteristic of a phase transition of the first order. The transition fields in the up and down sweep are tentatively defined as the points where the M shows a deviation from the nearly constant high value ($3.5-3.8\ \mu_B$/Mn site), and represented by H_C^+ and H_C^-, respectively.

For the M measurements, crystals were cut into cubes with the side length of about 2 mm. To estimate the absolute value of M with eliminating sample-shape dependence of sensitivity of the pickup coils, we carried out measurements also for powdered samples. The saturation moment M_0 was determined by an extrapolation of the M-H curve for $H > H_C^+$ to the zero field. The M_0 was estimated to be $3.5 \pm 0.2\ \mu_B$/Mn site at 1.4 K. This value is equal to the saturation moment of an average Mn ion moment ($3.5\ \mu_B$). Therefore, we can regard this highly magnetized state as a fully spin-polarized phase. The M-H curves are shown in Fig. 2 for various temperatures. The transition field decreases monotonously as T is increased, and the jump of M accompanied with hysteresis is no more visible at 274 K.

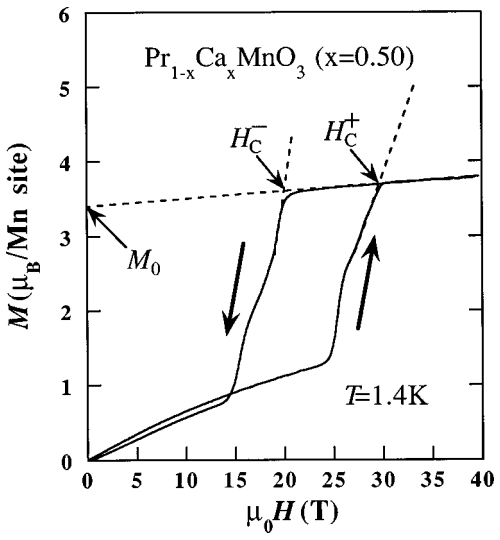

FIG. 1. M-H curve of a $Pr_{1-x}Ca_xMnO_3$ ($x=0.50$) single crystal at 1.4 K. Transition to the FM phase takes place at 30 T. Transition fields H_{CM}^+ and H_{CM}^- are defined as the saturation field of the M for up and down sweep, respectively.

Figure 3 shows the magnetic field (H) dependence of the resistivity (ρ) (longitudinal MR) of a $Pr_{1-x}Ca_xMnO_3$ ($x=0.50$) crystal at 117 K. The M-H curve at 123 K is also given by the dot-dashed line for comparison. Below the transition field, the ρ decreases only moderately with increasing H according to the enhancement of M. Negative MR effect takes place even in the insulating phase, and subsequently a

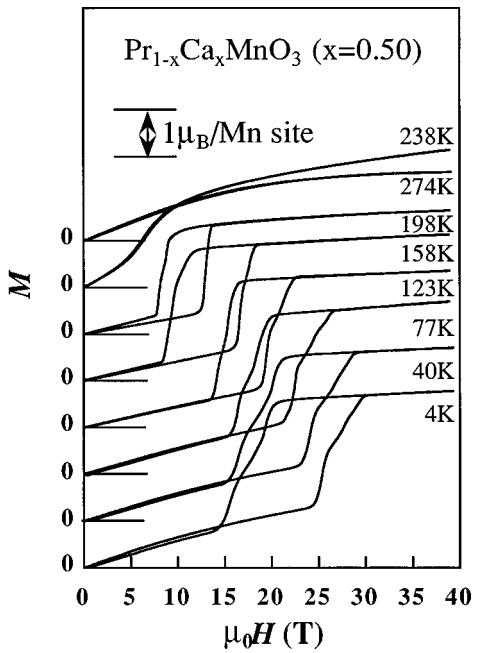

FIG. 2. Temperature dependence of the M-H curve of $Pr_{1-x}Ca_xMnO_3$ ($x=0.50$). Transition fields show monotonous decrease with increasing T. The transition width increases in low-temperature region.

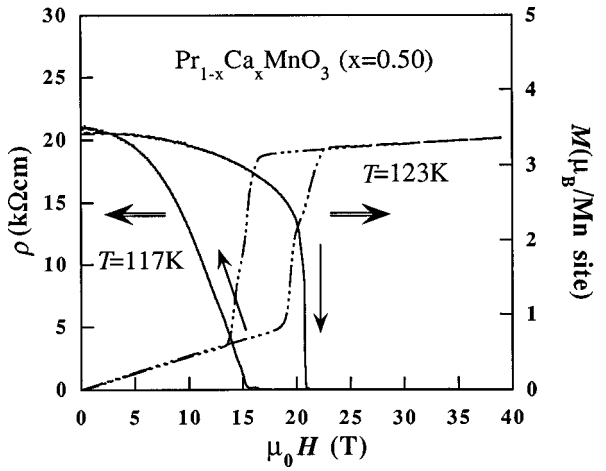

FIG. 3. Magnetoresistance of $Pr_{1-x}Ca_xMnO_3$ ($x=0.50$) at 117 K (solid line). M-H curve is also displayed by a dot-dashed line for comparison.

drastic change of ρ takes place at around 20 T.

Figure 4 depicts the phase diagram of $Pr_{1-x}Ca_xMnO_3$ ($x=0.50$) on the H-T plane. The open (closed) circles and squares represent $H_C^+(H_C^-)$ for samples 1 and 2, respectively. The hatched area represents the hysteretic region. There is no remarkable sample dependence in the phase diagram. The closed diamonds and crosses in Fig. 4 are the charge ordering temperature T_{CO} and the Néel temperature T_N determined by temperature dependence of ac susceptibility and magnetization under $\mu_0 H=8$ T. Both of these measurements were carried out in the warming process after the zero-field

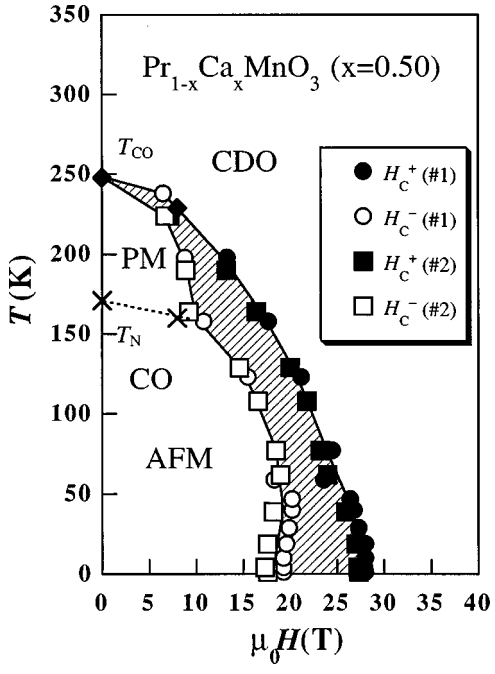

FIG. 4. Phase diagram in the H-T plane determined by the M and the MR measurements on two crystals of $Pr_{1-x}Ca_xMnO_3$ ($x=0.50$). Closed and open symbols stand for the critical fields determined from the up and down sweep of H, respectively. The hysteretic region is represented by a hatched area. The transition field increases with decreasing T and shows an anomaly at around T_N.

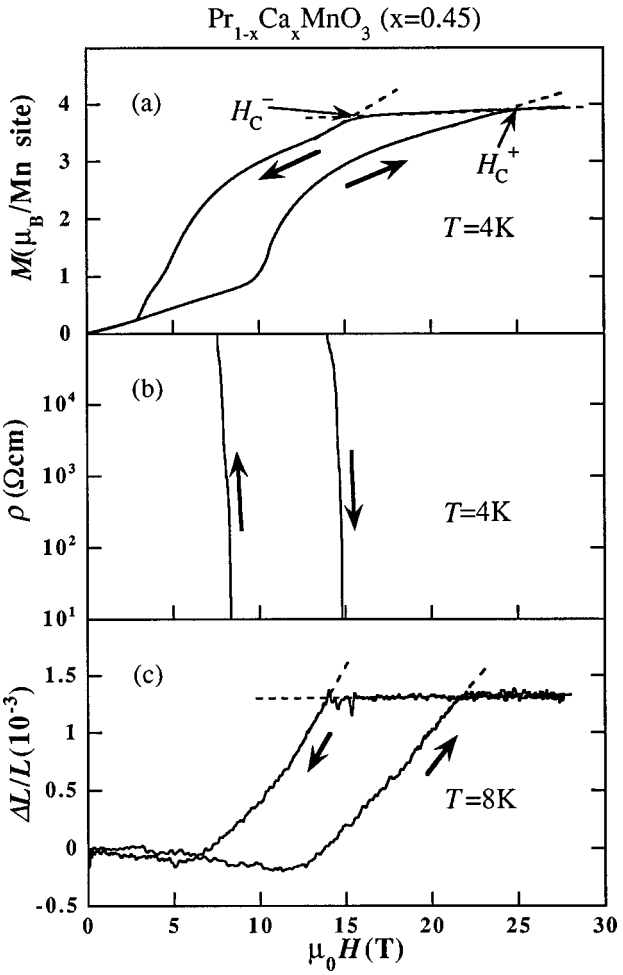

FIG. 5. (a) The magnetization (M) at 4 K (b) resistivity (ρ) at 4 K, and (c) magnetostriction ($\Delta L/L$) at 8 K for a $Pr_{1-x}Ca_xMnO_3$ ($x=0.45$) crystal are shown as a function of H. On the magnetic phase transition, CMR exceeding 4 orders of magnitude and MS in the order of 10^{-3} are observed.

cooling. In the region $T_N \leqslant T \leqslant T_{CO}$, the t_{2g} spins hold the paramagnetic (PM) state even in the CO phase. It is thus found from Fig. 4 that the profile of the CO phase boundary of $Pr_{1/2}Ca_{1/2}MnO_3$ is quite similar to those of $Nd_{1/2}Sr_{1/2}MnO_3$ (Ref. 12) and $Pr_{1/2}Sr_{1/2}MnO_3$.[13] However, the critical field to destroy the charge-ordered state becomes as high as 27 T at 1.4 K accompanying a large hysteresis. Reduction of the transition field with decreasing T in the low T region as reported for $x=0.35$ and 0.40 (Ref. 11) was not observed for $x=0.50$. On the other hand, the CO phase extends to higher H at temperatures below T_N.

The effect of the deviation of x from 0.50 on the charge-ordered state was studied in a $Pr_{1-x}Ca_xMnO_3$ ($x=0.45$) crystal. In addition to M and MR, MS has also been measured for a $x=0.45$ crystal in pulsed magnetic fields at various temperatures. All the samples used for the respective measurements were cut out of the same boule grown by the floating zone method. Figure 5(a) shows the M-H curve at 4 K. Below 10 T, the magnetization increases linearly with an increase in magnetic field. Successively, the M shows a steep increase at 10 T and saturates at 25 T. The onset field of the phase transition is much lower than that of the $x=0.50$ crystal. By contrast, the saturation field of M, does not show

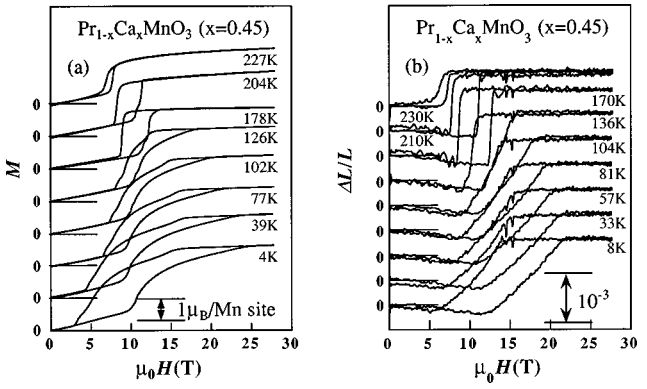

FIG. 6. (a) M-H and (b) $\Delta L/L$-H curves of $Pr_{1-x}Ca_xMnO_3$ ($x=0.45$) single crystals are compared at various temperatures. The structural phase transition is coupled with the magnetic phase transition. The transition is more gradual than in the $x=0.50$ sample. The transition width becomes narrower with increasing T.

such a remarkable difference between $x=0.45$ and 0.50. The transition fields H_C^+ and H_C^- were defined as the saturation fields in the same way as in the $x=0.50$ crystal. The ρ at 4 K is shown in Fig. 5(b) as a function of H. Because the resistance of the sample at relatively low magnetic field exceeds the range of the present measuring system, the result of the MR measurement is displayed with a limited dynamic range $10\ \Omega\ \text{cm}<\rho\leqslant 10^5\ \Omega\ \text{cm}$. The change in resistivity by 4 orders of magnitude takes place at around 14 T, which corresponds to the middle of the magnetic phase transition. The MS ($\Delta L/L$) at 8 K, defined as the relative change of the sample length along the direction of H, is shown in Fig. 5(c) as a function of H. In this figure, the data taken at 250 K is subtracted from the raw data to eliminate the background contribution. At $T=8$ K, the $\Delta L/L$ starts increasing at 12 T and reaches a value of $\sim 1.3\times 10^{-3}$ at 22 T. The observed large $\Delta L/L$ can be regarded as a manifestation of the structural transition rather than the ordinary MS.

The temperature variation of the M-H and $\Delta L/L$-H curves for the $x=0.45$ crystal is displayed in Fig. 6(a) and 6(b), respectively. It is evident from this figure that the structural phase transition is in accord with the magnetic phase transition. According to neutron-diffraction measurements by Jirák *et al.*,[10] the lattice constants of $Pr_{1-x}Ca_xMnO_3$ ($x=0.50$) have been reported as $a=5.395$ Å, $b=5.403$ Å, and $c=7.612$ Å at room temperature, and $a=5.430$ Å, $b=5.430$ Å, and $c=7.430$ Å at liquid He temperature. Therefore, this structural transition as detected by $\Delta L/L$ should reflect the recovering of the c-axis length. The transition fields show monotonous decrease with the increase of T. The width of the transition also decreases with increasing T, similarly to the case of $x=0.50$. Recently, Koshibae *et al.*[20] argued that the change in the magnetic structure induced by an external field may modify the pattern of orbital ordering in terms of a coupling between spin and orbital degrees of freedom. In the present case, the destruction of the orbital ordering by an external field gives rise to the structural phase transition and the recovering of the DE,which promotes the polarization of the t_{2g} spins.

The phase diagram of $Pr_{1-x}Ca_xMnO_3$ ($x=0.45$) determined by the magnetization measurements is displayed in Fig. 7. The temperatures of T_{CO} and T_N are determined by

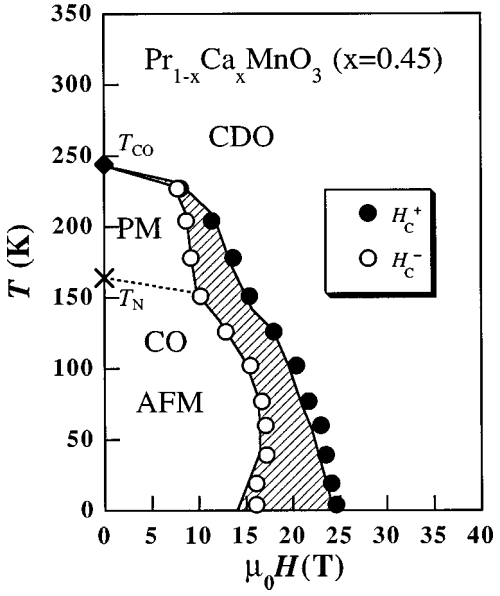

FIG. 7. The phase diagram of $Pr_{1-x}Ca_xMnO_3$ ($x=0.45$) determined by magnetization measurements. The shape of the phase boundary is similar to that of $x=0.50$ (Fig. 4).

the temperature dependence of ac susceptibility. It is noted that the CO phase boundary for $Pr_{1-x}Ca_xMnO_3$ ($x=0.45$) also shows an anomaly at T_N, and quite resembles that of $x=0.50$ rather than that of $x=0.40$.[11]

For the comparative study on the charge ordering transition in $R_{1-x}A_xMnO_3$, we have also investigated the x-dependent charge ordering phenomena for $Nd_{1-x}Ca_xMnO_3$ ($x=0.50$, 0.45, 0.40). The magnetization curves of these crystals at 4 K are displayed in Fig. 8. As shown in this figure, the onset field of the phase transition is decreased as x deviates from 0.50. In the M-H curve for $x=0.45$, the M increases steeply at about 12 T and then

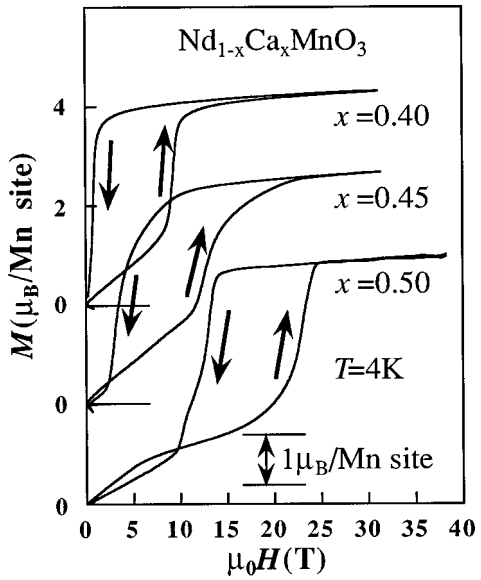

FIG. 8. M-H curves of $Nd_{1-x}Ca_xMnO_3$ ($x=0.50$, 0.45, and 0.40) at 4 K. The onset of the magnetic phase transition strongly depends on the x value. The saturation moment $M_0=4.4\pm 0.2\ \mu_B$ for $x=0.50$ is about $1\ \mu_B$ larger than the spin-only value of the Mn ion moment (see text).

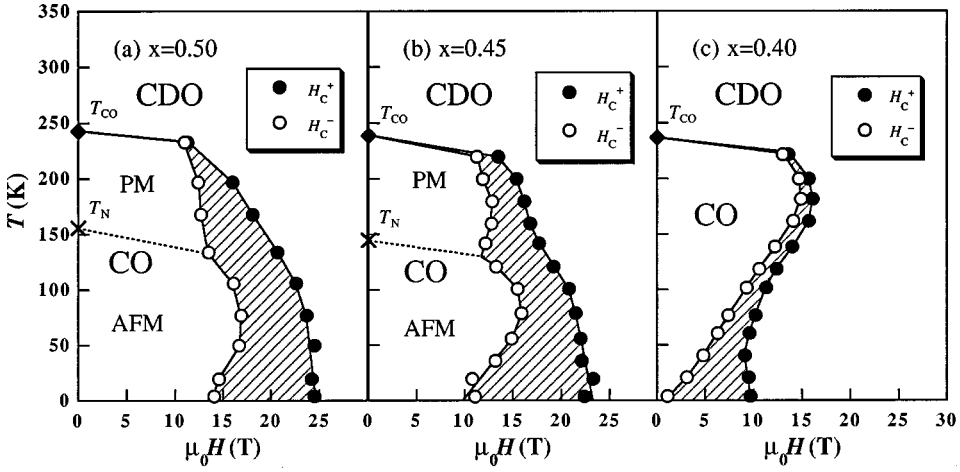

FIG. 9. The phase diagrams of $Nd_{1-x}Ca_xMnO_3$ for (a) $x=0.50$, (b) $x=0.45$, and (c) $x=0.40$ obtained from the magnetization measurements. The transition field exhibits a similar T dependence to that of the $Pr_{1-x}Ca_xMnO_3$ with the corresponding x (see Figs. 4 and 7 and Ref. 11).

gradually approaches the saturation moment, which is similar to the case of $Pr_{1-x}Ca_xMnO_3$ ($x=0.45$). For $x=0.40$, the transition field is the lowest and the metamagneticlike transition is clearly seen. The saturation moment of $Nd_{1-x}Ca_xMnO_3$ ($x=0.50$) estimated by the extrapolation of the M-H curve of the powdered sample to the zero field was $4.4\pm0.2\mu_B$. This value is about $1\mu_B$ larger than that of the $Pr_{1-x}Ca_xMnO_3$ ($x=0.50$). This extra moment originates perhaps from the field-induced Nd moment.

The phase diagrams for $Nd_{1-x}Ca_xMnO_3$ ($x=0.50$, 0.45, 0.40) are shown in Fig. 9. The thermodynamic transition field (H_C), which is tentatively defined as the average of H_C^+ and H_C^-, is estimated to be 19 T at 0 K for $x=0.50$, that is 4 T smaller than that of $Pr_{1-x}Ca_xMnO_3$ ($x=0.50$). In Fig. 9, the transition fields H_C^+ for $x=0.50$ and 0.45 show monotonous increase with decrease in temperature while that for $x=0.40$ decreases for $T<175$ K. Namely, the effect of deviation of x from 0.50 is pronounced for $x\leqslant0.40$, which resembles the case of $Pr_{1-x}Ca_xMnO_3$.[11]

IV. DISCUSSION

Temperature dependence of thermodynamic transition fields (H_C) of $R_{1-x}Ca_xMnO_3$ ($0.40\leqslant x\leqslant0.50$) for (a) $R=$Pr and (b) $R=$Nd is gleaned in Fig. 10 with the temperature normalized by T_{CO} in ordinate. The H_C value for $Pr_{1-x}Ca_xMnO_3$ ($x=0.40$) was quoted from literature.[11] In Figs. 10, the H_C's for both cases do not show remarkable x-dependent behavior at relatively high temperatures ($T/T_{CO}>0.7-0.8$). For low temperatures ($T/T_{CO}<0.7-0.8$), on the contrary, a significant variation of H_C with x appears. Consequently, dH_C/dT becomes positive at low temperatures for $x=0.40$, i.e., a reentrant-type phase boundary is realized. This is in sharp contrast with the case of $x=0.45$ and $x=0.50$ where the dH_C/dT remains negative even at low temperatures. The different profiles of the phase boundary between $x=0.40$ and $x=0.50$ (or 0.45) may be qualitatively explained as follows from a simple thermodynamic point of view.

According to the DE model,[21,22] the transfer integral t of e_g electrons between Mn^{3+} and Mn^{4+} ions is related to the relative angle θ of their localized t_{2g} spins,

$$t=t_0\cos(\theta/2), \tag{1}$$

where t_0 is the transfer integral in a fully spin-polarized state. The application of H tends to align the Mn t_{2g} spins via the Zeeman coupling, which leads to a decrease in θ and an increase in t. If kinetic energy of the charge carriers dominates over the CO instability, the insulator-metal transition takes place. Actually, application of H in the CO state causes negative MR effect even below the onset field of the transition as is seen in Fig. 3. This MR corresponds to the enhancement of t of the e_g carriers by the polarization of the localized t_{2g} spins.

In $Pr_{1-x}Ca_xMnO_3$, the deviation of x from 0.5 has been argued in terms of the modification of the AFM CE-type

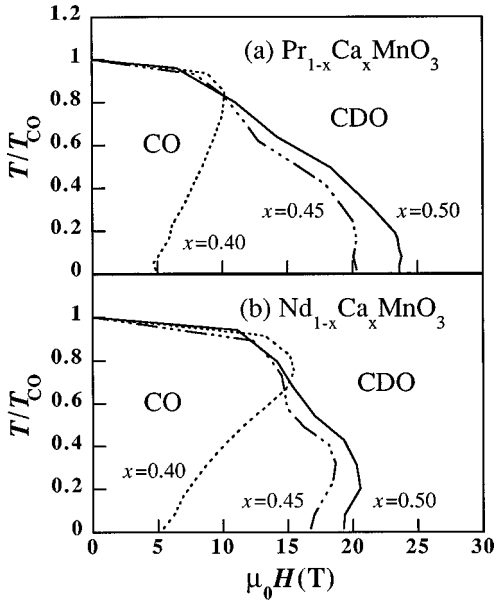

FIG. 10. Temperature dependence of the thermodynamic transition fields (H_C) of $R_{1-x}Ca_xMnO_3$ ($0.40\leqslant x\leqslant0.50$) for (a) $R=$Pr and (b) $R=$Nd. The temperature is normalized by T_{CO}. For $Pr_{1-x}Ca_xMnO_3$ ($x=0.40$), the H_C is quoted from the literature (Ref. 11).

structure. For $x=0.5$, the arrangement of spins along the orthorhombic c axis is antiferromagnetic while for $x<0.5$ it is canted (for $x=0.3$ it becomes ferromagnetic) although the CE-type ordering is kept within the ab plane. As postulated by Jirák *et al.*,[10] such a modification of the spin structure has been discussed in terms of the extra carriers that promote the DE along the c direction. The extension of the wave function of the e_g electrons generated in the CO state can mediate the DE between the neighboring t_{2g} spins along the c axis, which leads to the canted AFM state, so that θ becomes smaller than 180° at low temperatures. Such an effect of the deviation from $x=0.50$ on the magnetic structure should result in smaller transition fields especially at low temperatures, in accord with the observation.

At a finite temperature, the transition field is determined by the Helmholtz's free energy F, which is expressed as $F=U\text{-}TS\text{-}MH$. Here, U denotes the internal energy and S the entropy. As mentioned before, $dH_C/dT>0$ at low temperatures for $x=0.40$, whereas $dH_C/dT<0$ for $x=0.45$ and $x=0.50$. The point here is that the CO state for $x=0.50$ may have a smaller S than that for $x=0.40$, since the latter possesses excess carriers due to the discommensuration. The commensurate CO significantly freezes the kinetic and the orbital degrees of freedom of the e_g electrons especially at low temperatures. The larger S in the discommensurate CO state leads to the larger dH_C/dT than that in the commensurate case. Although the reasons for $dH_C/dT<0$ for $x=0.50$ and $x=0.45$ are unknown as yet, the difference in the temperature dependence of transition fields between the $x=0.50$ and $x=0.40$ crystal can thus be qualitatively explained by the difference of the entropy term S in the CO state or be due to field-induced changes in the electronic states.[23]

V. CONCLUSION

We have found that even the commensurate charge ordering of $Pr_{1-x}Ca_xMnO_3$ and $Nd_{1-x}Ca_xMnO_3$ with $x=0.50$ is destroyed by applying magnetic fields up to 40 T. The transition fields of the charge-ordered phases of $x=0.45$ and 0.50 decrease monotonously as temperature is increased, which is in remarkable contrast with the case of $x=0.40$ with a larger discommensuration. The different temperature dependence of the transition fields at low temperatures between $x=0.50$ and 0.40 can be qualitatively explained in terms of the excess entropy of the nearly localized e_g electrons which are introduced by the deviation from $x=0.50$ in the charge-ordered state. The phase diagrams suggest that the co-linear CE-type antiferromagnetic ordering of the localized Mn spins plays an important role in the stabilization of the charge-ordered state. The colossal magnetoresistance effect due to the destruction of the charge ordering is accompanied by the structural phase transition in addition to the magnetic phase transition. This result implies that the destruction of the orbital ordering is a key factor in the colossal magnetoresistance of the manganites.

ACKNOWLEDGMENTS

The authors would like to thank K. Koui, M. I. Bartashevich, and T. Goto for their help in carrying out magnetostriction, ac susceptibility, and isofield magnetization measurements. The authors would like also to thank N. Nonose for the inductively-coupled plasma mass spectrometry measurements. This work was in part supported by the New Energy and Industrial Technology Development Organization (NEDO) and also by a Grant-In-Aide for Scientific Research from the Ministry of Education, Science and Culture, Japan.

*Present address: The Institute of Physical and Chemical Research (RIKEN), Wako, Saitama 351-01, Japan.

[1] R. M. Kusters, J. Singleton, D. A. Keen, R. McGreevy, and W. Hayes, Physica B **155**, 362 (1989).

[2] K. Chahara, T. Ohno, M. Kasai, and Y. Kozono, Appl. Phys. Lett. **63**, 1990 (1993).

[3] S. Jin, T. H. Tiefel, M. McCormack, R. A. Fastnacht, R. Ramesh, and L. H. Chen, Science **264**, 413 (1994); M. McCormack, S. Jin, T. H. Tiefel, R. M. Fleming, and Julia M. Phillips, Appl. Phys. Lett. **64**, 3045 (1994).

[4] Y. Tokura, A. Urushibara, Y. Moritomo, T. Arima, A. Asamitsu, G. Kido, and N. Furukawa, J. Phys. Soc. Jpn. **63**, 3931 (1994); A. Urushibara, Y. Moritomo, T. Arima, A. Asamitsu, G. Kido, and Y. Tokura, Phys. Rev. B **51**, 14 103 (1995).

[5] H. L. Ju, C. Kwon, Qi Li, R. L. Greene, and T. Venkatesan, Appl. Phys. Lett. **65**, 2108 (1994).

[6] R. v. Helmolt, J. Wecker, K. Samwer, and K. Bärner, J. Magn. Magn. Mater. **151**, 411 (1995).

[7] G. H. Jonker, Physica (Amsterdam) **XVI**, 337 (1950); J. B. Goodenogh and J. M. Longo, in *Magnetic and Other Properties of Oxides and Related Compounds*, edited by K.-H. Hellwege and A. M. Hellwege (Springer-Verlag, Berlin, 1970), p. 126.

[8] H. Yoshizawa, H. Kawano, Y. Tomioka, and Y. Tokura, Phys. Rev. B **52**, 13 145 (1995).

[9] E. O. Wollan and W. C. Koehler, Phys. Rev. **100**, 545 (1955).

[10] Z. Jirák, S. Krupička, Z. Šimša, M. Dlouhá, and S. Vratislav, J. Magn. Magn. Mater. **53**, 153 (1985).

[11] Y. Tomioka, A. Asamitsu, H. Kuwahara, Y. Moritomo, and Y. Tokura, Phys. Rev. B **53**, 1689 (1996).

[12] H. Kuwahara, Y. Tomioka, A. Asamitsu, Y. Moritomo, and Y. Tokura, Science **270**, 961 (1995).

[13] Y. Tomioka, A. Asamitsu, Y. Moritomo, H. Kuwahara, and Y. Tokura, Phys. Rev. Lett. **74**, 5108 (1995).

[14] E. Pollert, S. Krupička, and E. Kuzmičová, J. Phys. Chem. Solids **43**, 1137 (1982).

[15] Z. Jirák, E. Pollert, A. F. Andresen, J. C. Grenier, and P. Hagenmuller, Eur. J. Solid State Inorg. Chem. **27**, 421 (1990).

[16] C. Brist and M. Lucco-Borlera, J. Inorg. Nucl. Chem. **27**, 2129 (1965); N. Mizutani, A. Kitazawa, N. Ohkuma, and H. Kato, Kogyo Kagaku Zasshi **73**, 1097 (1970).

[17] S. Takeyama, H. Ochimizu, S. Sasaki, and N. Miura, Meas. Sci. Technol. **3**, 662 (1992).

[18] N. Yamada, S. Takeyama, T. Sakakibara, T. Goto, and N. Miura, Phys. Rev. B **34**, 4121 (1986).

[19] G. Kido, Physica B **155**, 199 (1989).

[20] W. Koshibae, Y. Kawamura, S. Ishihara, S. Okamoto, J. Inoue, and S. Maekawa (unpublished).

[21] P. W. Anderson and H. Hasegawa, Phys. Rev. **100**, 675 (1955).

[22] P.-G. de Gennes, Phys. Rev. **118**, 141 (1960).

[23] J. L. Pichard, M. Sanquer, K. Slevin, and P. Debray, Phys. Rev. Lett. **65**, 1812 (1990).